

Effects of nearshore recharge on groundwater interactions with a lake in mantled karst terrain

Terrie M. Lee

U.S. Geological Survey, Tampa, Florida

Abstract. The recharge and discharge of groundwater were investigated for a lake basin in the mantled karst terrain of central Florida to determine the relative importance of transient groundwater inflow to the lake water budget. Variably saturated groundwater flow modeling simulated water table responses observed beneath two hillsides radiating outward from the groundwater flow-through lake. Modeling results indicated that transient water table mounding and groundwater flow reversals in the nearshore region following large daily rainfall events generated most of the net groundwater inflow to the lake. Simulated daily groundwater inflow was greatest following water table mounding near the lake, not following subsequent peaks in the water level of upper basin wells. Transient mounding generated net groundwater inflow to the lake, that is, groundwater inflow in excess of the outflow occurring through the deeper lake bottom. The timing of the modeled net groundwater inflow agreed with an independent lake water budget; however, the quantity was considerably less than the budget-derived value.

1. Introduction

Groundwater inflow generated by temporary flow patterns in the water table adjacent to lakes can have a noticeable effect on lake geochemistry and hydrology [Anderson and Munter, 1981; Winter, 1983; Katz *et al.*, 1995; Krabbenhoft and Webster, 1995; Winter and Rosenberry, 1995; Lee and Swancar, 1997]. However, the actual amount of groundwater recharge and discharge associated with these temporary flow patterns remains poorly understood. Highly transient features in the water table such as seepage faces and water table mounds or troughs occur primarily near the shoreline of surface waters. In this area the water table is often sufficiently close to land surface to be rapidly and efficiently recharged by rainfall and to be lowered by evapotranspiration losses [Novakowski and Gillham, 1988; Salvucci and Entekhabi, 1995]. The distance from a lake considered to be the nearshore region, and the time that transient flow patterns last, depends upon both the physical characteristics of the basin (topographic relief, soil properties, and hydrogeologic setting) and climate [e.g., Winter, 1983]. Previous studies have described transient water table fluctuations in the relatively low permeability aquifers surrounding prairie potholes and wetlands of North Dakota and Canada [Meyboom, 1966; Winter and Rosenberry, 1995; Rosenberry and Winter, 1997]. Relatively few studies have described transient groundwater flow patterns around lakes in the sandy, coastal deposits and mantled karst terrain of the humid southeastern United States [Lee and Swancar, 1997].

At present, the distinctive hydrology of the nearshore region of lakes is difficult to describe within a context of basin-scale processes. Studies that simulate the interaction between a lake and the surrounding groundwater basin typically rely on saturated groundwater flow models that do not include the effect of the unsaturated zone on recharge. Thus saturated flow models cannot simulate the rapid and small-scale transient ground-

water flow processes observed in the nearshore region and integrate them with flow in the rest of the basin. As a result, it is difficult to simulate how much of the total groundwater inflow to surface waters is coming from the nearshore region. A detailed lake water budget, however, can provide evidence for transient groundwater flows that are not simulated by saturated flow modeling. At Lake Barco, a seepage lake in northern Florida, a monthly lake water budget revealed rapid increases in the groundwater inflow to the lake on rainy months. However, these increases were not simulated in a transient, saturated, groundwater-flow model of the lake basin. Because the model closely predicted water levels observed farther from the lake, the results implicated the nearshore region as a significant source of the groundwater inflow to the lake in these months [Lee, 1996].

Combining lake water-budget studies with variably saturated flow modeling of lake basins provides an approach for studying the connection between climate, topography, geologic setting, and groundwater discharge to lakes. A two-dimensional (2-D) hillside provides an extremely useful image for envisioning subsurface flow processes on a basin scale, and it offers a simpler alternative to the three-dimensional counterpart [Winter, 1983; Winter, 1988; Salvucci and Entekhabi, 1995]. Variably saturated flow modeling remains more hypothetical than quantitative because of our limited ability to describe the spatial and temporal distribution of hydrologic parameters across basins. Nevertheless, it integrates recharge and discharge in the nearshore region and the greater basin and provides a tool to refine concepts about lake and groundwater interactions. Variably saturated flow models have been used to simulate transient flow phenomena in hypothetical or real basins [Freeze, 1971; Winter, 1983; Mills and Zwarich, 1986; Potter and Gburek, 1988; Stolte *et al.*, 1992]. However, in only a few studies have researchers purposefully instrumented the nearshore region of a lake to examine transient groundwater flow patterns in detail [e.g., Rosenberry and Winter, 1997]. Fewer still have simulated field observations using a variably saturated flow model.

This paper describes (1) the groundwater flow patterns in the nearshore area of Lake Barco, a seepage lake in Florida's

This paper is not subject to U.S. copyright. Published in 2000 by the American Geophysical Union.

Paper number 2000WR900107.

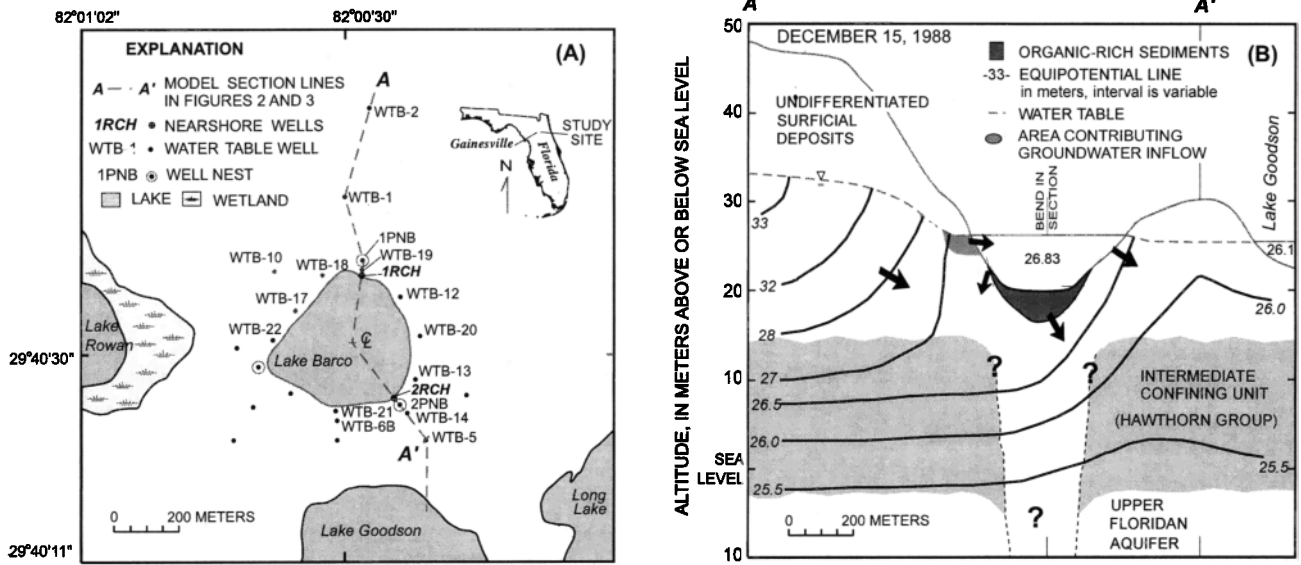


Figure 1. Groundwater flow pattern in the Lake Barco basin for December 15, 1988. (a) Areal view showing location of monitor wells and position of section line shown in the vertical view. (b) Vertical view showing groundwater flow pattern and topography along section line A-A'. (c) Areal view showing areas of groundwater inflow and lake leakage (modified from Lee [1996]).

Central Lake District, (2) the results of simulating transient water table mounding in the nearshore area using variably saturated flow modeling, and (3) the predicted effect of nearshore recharge on the timing and magnitude of groundwater exchange with the lake. Groundwater levels were monitored continuously in the nearshore region and periodically in wells farther from the lake, termed basin wells hereinafter. A 2-D, variably saturated groundwater flow model was used to simulate the equilibrium and transient water table configurations along two hillsides in the lake basin: an “inflow” hillside with a water table sloping toward the lake and an “outflow” hillside with a water table sloping away from the lake. Modeled fluxes were compared to net groundwater flow computed by a monthly water budget of the lake. Both lines of evidence were

used to infer the relative importance of nearshore recharge to the water budget of the lake.

1.1. Site Description

Lake Barco lies in the northern part of the Central Lake District of peninsular Florida, an upland region of discontinuous sandy ridges dotted with more than 3000 lakes [Brooks, 1981]. Lake Barco is small (11.7 ha), nearly circular, and has a maximum depth of 6.7 m at a stage of 26.70 m above sea level [Sacks et al., 1992] (Figure 1). The mantled karst terrain around Lake Barco is characterized by sinkholes and solution-basin lakes formed by the piping of sand and clay mantle deposits into solution voids in the underlying limestone [Arrington and Lindquist, 1987]. The sandy surficial deposits contain the surficial aquifer and the lake [Sacks et al., 1992]. These deposits overlie a clay-rich formation containing the intermediate confining unit (Figure 1b) [Scott, 1983]. This unit confines or partially confines the underlying Upper Floridan aquifer, a massive sequence of transmissive limestone. The climate at Lake Barco is humid subtropical, with a mean annual rainfall (1961–1990) of 131.6 cm at the Gainesville Municipal Airport, about 26 km west of Lake Barco [National Oceanographic and Atmospheric Administration, 1996]. During 1996, rainfall at Lake Barco was 12.3 cm greater than the average, largely attributable to March rainfall that was 19.7 cm greater than average. The infiltration rate of the sandy soil is extremely high [Readle, 1990], and the basin generates little to no surface runoff.

1.2. Groundwater Setting

Lake Barco is in a flow-through setting with respect to groundwater flow in the surficial aquifer. For average annual rainfall conditions, groundwater flows in along the lake’s northern margin, and lake water leaks out along the southern shoreline (Figure 1c). During dry periods, lake leakage can extend northward along both sides of the lake, and particularly along the western margin, until inflow is restricted to the north-

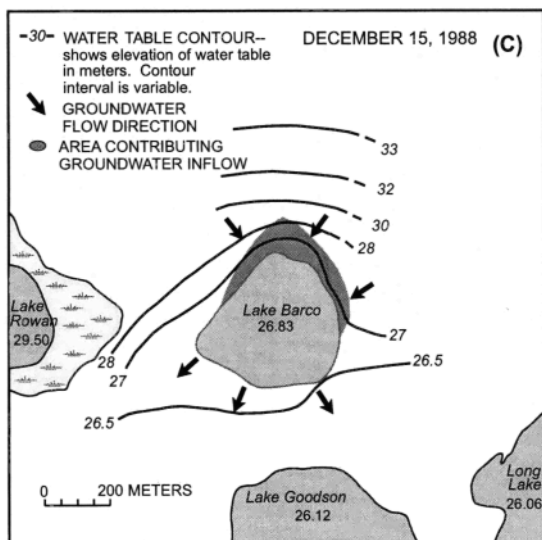


Figure 1. (continued)

eastern shoreline [Sacks *et al.*, 1992]. The surficial aquifer naturally recharges the Upper Floridan aquifer in this setting, and the recharge rate is magnified where karst subsidence features breach the confining unit. This tendency for downward flow has the effect of reducing the extent of the surficial aquifer contributing lateral groundwater inflow to the lake. Although the water table contours are higher than the lake throughout the northern basin, the simulated steady state ground watershed for Lake Barco is a small, crescent-shaped area extending outward about 100 m from the northern shore [Lee, 1996] (Figure 1c). Flow originating farther away from the lake travels too deep within the surficial aquifer to be intercepted by the lake bed (Figure 1b).

2. Methods

2.1. Hydrologic Monitoring

Groundwater levels in the surficial aquifer around Lake Barco were monitored in an existing network of wells described by Sacks *et al.* [1992] and shown in Figure 1a. Near the edge of the lake the water table was monitored at two "recharge" sites, 1RCH and 2RCH (Figure 1a). At each RCH site, three wells were installed along a line perpendicular to the shoreline. An "A" well was finished below the lake bed at about 2 to 5 m offshore, where the lake was less than about 0.3 m deep. A second well, "B", was drilled about 2.5 to 5 m onshore where the water table was estimated to be about 0.3 m below land surface and where one might expect a seepage face to form. The "C" well was drilled from 7 to 18 m onshore, where the water table was expected to be about 0.5 m below the land surface and no seepage face was expected to occur. Wells were augered and then backfilled with cuttings. Well casings were made of 5-cm-diameter PVC with a small screened interval (0.76 or 0.91 m) and were finished about 1 m below the water table.

Between September 1995 and December 1996, water levels were measured weekly in the six nearshore wells and in four basin wells that were also close to the lake. All of the wells in the basin were measured biweekly, and results were used to construct water table contour maps. Between March and May of 1996, water levels at 1RCH and 2RCH also were monitored at 15-min intervals using pressure transducers. The resulting 3 months of continuous data captured extremes in both wet and dry conditions. March, with 29 cm of rainfall, had more than 3 times the long-term monthly average of 9.27 cm and was the wettest month of 1996. April rainfall (5.64 cm) was close to the monthly average (6.71 cm), and May was dry (3.08 cm compared with 9.55 cm average).

Lake stage and rainfall were monitored between July 1995 and December 31, 1996. Lake stage was read weekly from staff gages at Lake Barco and Lake Rowan, and weekly cumulative rainfall was measured using a storage rain gage. Continuous lake stage and rainfall data were collected every 15 min beginning January 13, 1996. Data collection methods were similar to those described in earlier papers [Pollman *et al.*, 1991; Sacks *et al.*, 1992].

Hydrologic data were used to construct a water budget for Lake Barco and to derive monthly net groundwater flow to the lake in the manner described by Sacks *et al.* [1992]. Months with positive net groundwater flow indicated that groundwater inflow to the lake was greater than lake leakage during the month. A negative value of net groundwater flow indicated that lake leakage exceeded groundwater inflow.

For the lake water budget, monthly evaporation losses were based upon 1996 pan evaporation data from a National Oceanic and Atmospheric Administration site in Gainesville about 40 km west of Lake Barco. These data were corrected with monthly pan coefficients developed for Lake Barco in 1990 using an energy-budget evaporation analysis [Sacks *et al.*, 1994]. The lake stage-volume and stage-area curves needed to compute lake area and the change in storage terms were from Sacks *et al.* [1992]. Error estimates for the monthly budget terms were chosen to be conservative. Evaporation errors were assumed to be $\pm 20\%$ of the estimated evaporation value. The error in monthly rainfall was $\pm 10\%$ and was $\pm 5\%$ for the change in lake volume.

2.2. Numerical Modeling of Variably Saturated Flow

2.2.1. Model theory and assumptions. Variably saturated flow was simulated using the HYDRUS-2D flow model [Šimůnek *et al.*, 1996]. At the core of HYDRUS-2D is the computer program SWMS_2D, a two-dimensional, finite element model which numerically solves the Richards' equation for unsaturated-saturated water flow in porous media and the Fickian-based convection-dispersion equation for solute transport [Šimůnek *et al.*, 1992]. The merit of SWMS_2D is reviewed by Gribb and Sewell [1998]. HYDRUS-2D unites this earlier code with a sophisticated graphical user interface. The model assumes two-dimensional, isothermal, Darcian flow of water in a variably saturated rigid porous media. It also assumes that air flow is insignificant. The governing flow equation for variably saturated flow is Richards' equation as applied by Šimůnek *et al.* [1996]:

$$\frac{\partial \theta}{\partial t} = \frac{\partial}{\partial x_i} \left[K \left(K_y^A \frac{\partial h}{\partial x_j} + K_z^A \right) \right] - S, \quad (1)$$

where θ is the volumetric water content [$L^3 L^{-3}$], h is the pressure head [L], S is a sink term [T^{-1}], x_i ($i = 1, 2$) are the spatial coordinates [L], t is time [T], and K_y^A are the components of a dimensionless anisotropy tensor \mathbf{K}^A used to account for an anisotropic medium. K is the unsaturated hydraulic conductivity function [$L T^{-1}$] given by

$$K(h, x, z, t) = K_s(x, z) K_r(h, x, z, t), \quad (2)$$

where K_s is saturated hydraulic conductivity and K_r is relative hydraulic conductivity [$L T^{-1}$].

If (1) is applied to planar flow in a vertical cross section, $x_1 = x$ is the horizontal dimension and $x_2 = z$ is the vertical dimension, assumed positive upward. For flow in an axisymmetric system, $x_1 = r$, where r is the radial distance from the centerline.

2.2.2. Radial models. Lake Barco and its basin were conceptualized as being circular. Two radial models were then used to represent the subsurface flow beneath the two halves of the basin: the northern or inflow half and the southern or outflow half. The section line that traces the inflow and outflow hillsides is shown on Figure 1a. The models of the inflow and outflow hillsides are shown in Figures 2 and 3. The inflow hillside extends 800 m from the center of the lake bottom (elevation 20.12 m) to the topographic drainage divide (48 m), which was also the groundwater flow divide (Figures 1b and 2). The outflow hillside rises to the top of a much lower ridge south of the lake (Figure 3). This low ridge separates Lake Barco on the north from Lake Goodson to the south. The ridge overlies a trough in the water table caused by a karst subsi-

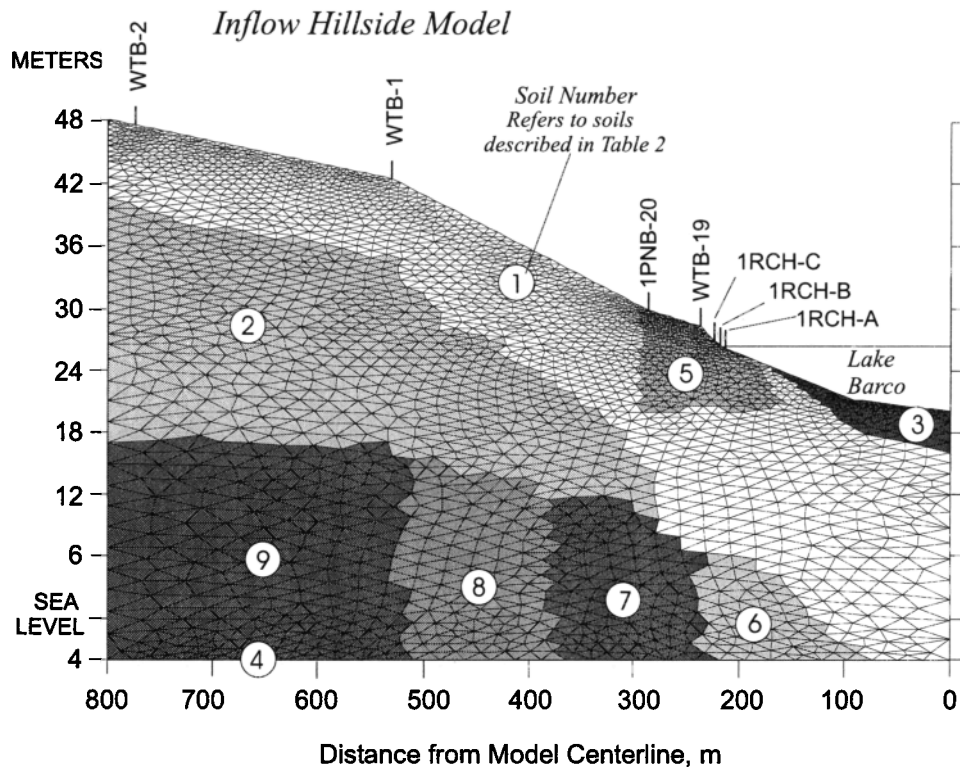


Figure 2. Northern (inflow) hillside model showing finite element mesh, soil numbers, and location of observation wells. (Note that Figure 2 is shown in mirror image for ease of comparison with Figure 1. In actual numerical simulation the origin is at the lower, left-hand corner of the model domain.)

dence feature that enhances downward leakage in this area [Sacks *et al.*, 1992; Lee, 1996] (Figures 1b and 1c).

The finite element mesh for each model was generated using a mesh generator algorithm within HYDRUS-2D [Šimůnek *et al.*, 1996]. For both models the vertical dimension of the mesh elements near the lake margin was between 10 and 20 cm, with horizontal dimensions between 3 and 5 m. Element dimensions in both models increased gradually with depth and distance from the lake and were largest in the saturated zone of the intermediate confining unit, where velocities were low (Figures 2 and 3). To attain the necessary vertical to horizontal distortion in each mesh, the mesh anisotropy variable, $\Delta z/\Delta h$, was specified as 0.04.

2.2.3. Model boundaries. Model boundaries used in this study followed the saturated flow model boundaries described by Lee [1996]. The lateral boundaries for both models were no-flow boundaries and occurred where the flow in the unsaturated and saturated zones was predominantly vertical. The lower model boundaries coincided with the top of the transmissive Upper Floridan aquifer and were assigned a specified pressure head. During the transient simulation period the observed head in the Upper Floridan aquifer was roughly constant and varied less than ± 0.25 m from the specified boundary head value.

2.2.3.1. Steady state simulations: Where the lake submerged the lower hillside, the boundary along the hillside was a specified pressure head. Pressure head values were distrib-

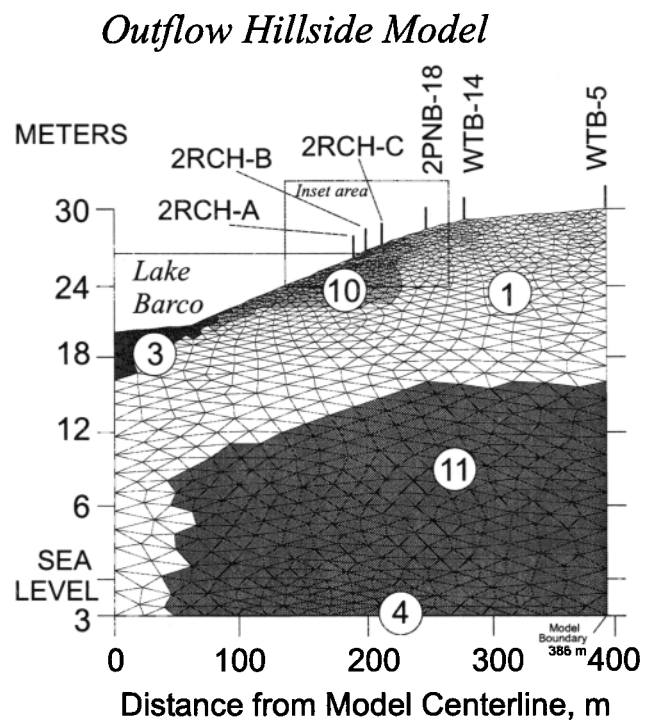


Figure 3. Southern (outflow) hillside model showing finite element mesh, soil numbers, and location of observation wells. Inset area shown in Figure 8.

uted spatially to reflect hydrostatic conditions of the lake stage. The remaining hillside was a constant flux boundary that received a uniform recharge rate of 0.108 cm/d or about 30% of the average annual rainfall. This rate was based on an annual average recharge efficiency estimated from the chloride mass balance of the shallow groundwater at Lake Barco [Pollman *et al.*, 1991; Lee, 1996]. Simulations were run with and without a seepage face next to the lake. Lake and groundwater levels observed in the Lake Barco basin on December 15, 1988, were considered representative of steady state conditions [Lee, 1996].

2.2.3.2. Transient simulations: The water table position below each hillside was simulated daily for the 3-month period March through May 1996. Transient simulations were begun 4 months before March, on October 31, 1995, to diminish the effect of the initial conditions on the period of interest. The steady state pressure head distribution for each model provided the initial condition and was similar to the observed lake and groundwater levels on October 31, 1995. The 4-month period between October 31, 1995, and February 27, 1996, was simulated using weekly average values for boundary variables. For the next 3 months, boundary conditions were typically redefined daily.

A daily net recharge rate was applied to the upper hillsides beyond the nearshore region. The daily net recharge was derived with an empirical relationship defined by Lee [1996] that attributes most net recharge to large daily rainfall events. Daily net recharge was estimated to equal 40% of the daily rainfall in excess of 0.64 cm (0.25 inch), while daily rainfall less than 0.64 cm produced no net recharge. The sum of daily net recharge computed in this manner produced an annual net recharge rate similar to the long-term average estimate of 30%. For example, the sum of daily net recharge computed in the manner above was about 39 cm or 27% of the annual total rainfall of 144 cm in 1996. These recharge estimates may be conservatively low, particularly for a year with above average rainfall. For average rainfall conditions, annual net recharge in ridge areas of central Florida has been estimated to range from 30–40% of annual rainfall [Knowles, 1996] to 43–53% [Sumner, 1996].

The daily net recharge rate was applied as a time-varying specified flux along the upper hillside of each model. It was applied starting where the thickness of the unsaturated zone was about 2.5 m or greater (near sites 1PNB and 2PNB) (Figures 2 and 3, respectively). While this approach maintains the long-term water balance in the upper reaches of the basin, it is unlikely to reflect the short-term water balance in the unsaturated zone or short-term water level changes. However, this simplification was considered acceptable because water levels in the upper basin responded relatively slowly (as viewed during the 3-month simulation period) to an aggregate of rainfall events in contrast to the nearshore region where water levels showed an immediate response to individual rainstorms. Thus, for these transient simulations, recharge in the upper basin provided reasonable heads over time, effecting a general head boundary to the nearshore region.

Near the edge of Lake Barco, where the unsaturated zone was thinner than about 2.5 m, daily recharge was assumed to be most of the daily rainfall [Wu *et al.*, 1996]. The rapid, steep, water table mounding observed in the nearshore region could not be simulated using the recharge rate applied to the upper hillside, regardless of the assumed soil moisture characteristics. Evaporation from the soil was simulated, but transpiration was not, although the effect of this simplification is discussed. The monthly average evaporation rates for Lake Barco in 1990

provided the maximum allowable evaporation rates from the soil surface (0.25 cm/d in March and the preceding 4 months, 0.33 cm/d in April, and 0.44 cm/d in May) [Sacks *et al.*, 1994].

Recharge in the nearshore region was expected to best reflect conditions near the two RCH sites where the depth to water was typically 1.5 m or less, and to overpredict short-term recharge where the water table depth was greater (between 1.5 and 2.5 m). Actual recharge should vary as a function of the depth to the water table. Simplifying the recharge along the hillside into two zones with respect to water table depth was considered to be sufficient for testing the desired hypotheses. It was also necessary to meet the limits in the number of different time-varying boundary conditions currently handled by the model.

The pressure head distribution along the lake bed was varied approximately daily throughout the transient simulations to reflect the observed lake stage. Boundary nodes were re-assigned to be lake or emergent hillside as necessary to accommodate the changing stage. Transient simulation of the lake boundary condition was an adaptation of the original model code made for this study (J. Šimůnek, Salinity Laboratory, U.S. Department of Agriculture, Riverside, California, written communication, December 1996). No seepage face was used in the transient simulations; however, the effect of a seepage face on the steady state simulation results is discussed in section 3.3.1.

2.2.4. Soil characteristics. The soil in the Lake Barco basin is composed of mostly fine- to medium-grained sand with a small fraction of silt and clay. On the inflow side at site 1PNB (about 60 m from 1RCH-C), soils to a depth of 15 m were over 99% sand, and silt and clay size fractions made up less than 1%. On the outflow side at site 2PNB (about 30 m from 2RCH-C), soils were 95–98% sand with 2–5% of silt and clay.

The unsaturated soil characteristics at Lake Barco were not measured directly. Instead, the model uses data for a similar Candler series sand (deeply weathered, acidic, uncoated, Typic Quartzipsamments) collected at a site in Orange County about 160 km farther south in the Central Lake District [Readle, 1990; Sumner, 1996; D. Sumner, U.S. Geological Survey, Altamonte Springs, Florida, written communication, 1996]. Soil water retention was measured over the drying phase, and data were fit to a soil moisture characteristic curve based on the equations of *van Genuchten et al.* [1991]. The results for a 30-cm-deep soil sample are shown in Figure 4a. This soil was used to represent the upper surficial deposits at Lake Barco (see soil number 1 in Figures 2 and 3). Clay content in the surficial deposits typically increased with depth. Therefore the lower surficial deposits in the inflow model (soil number 2 in Figure 2) were assumed to be clayey sand described by *Sumner and Bradner* [1996] (Figure 4b).

Below the elevation of the lake surface, porous media in the model were typically saturated, and horizontal hydraulic conductivity (K_x) and anisotropy were the only soil parameters required. Initial values of K_x and anisotropy for the surficial aquifer and the intermediate confining unit were from the saturated flow model of Lake Barco [Lee, 1996]. The anisotropy in the saturated zone was 10. An anisotropy of 1 was assumed in the unsaturated zone.

3. Results

3.1. Measured Water Table Responses to Recharge

Rainfall caused rapid mounding in the water table near the edge of Lake Barco. The water table rose equally quickly on

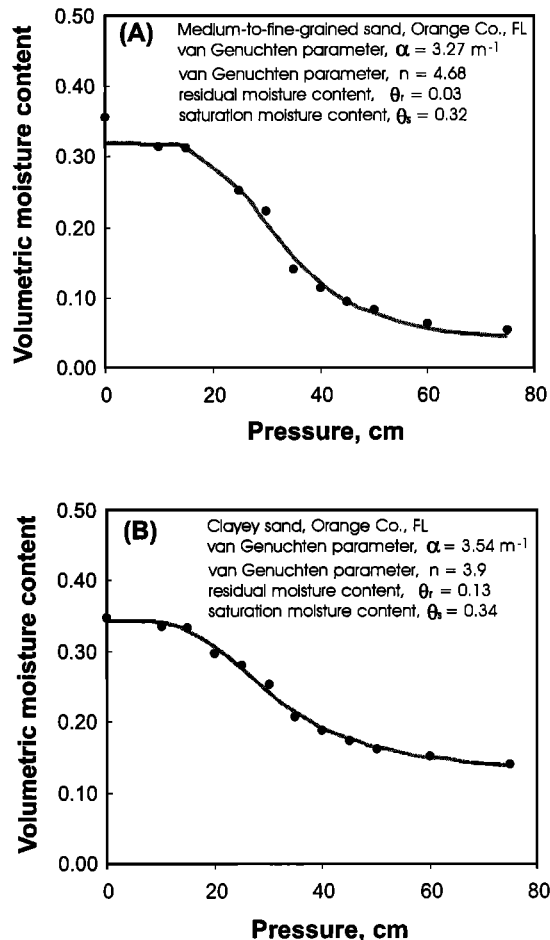


Figure 4. Soil moisture characteristic curves for two soils used in hillside models: (a) sand and (b) clayey sand. Both soils were collected in Orange County, Florida. Data were fit to the van Genuchten *et al.* [1991] formulation.

the inflow and outflow sides of the lake but subsided more rapidly on the inflow side. In fact, on the inflow side, water table mounding was not apparent if water levels were viewed only once daily. On a daily basis, water levels in wells 1RCH-A, 1RCH-B, and 1RCH-C were consistently above lake stage and tracked one another uniformly, revealing a low inflow head gradient toward the lake that increased slightly on days with rainfall (Plate 1a). Transient mounding became clearly evident in the 15-min water level measurements. For example, on March 18, 1996, 6.89 cm of rain fell within 3.5 hours. Recharge and recovery were both so rapid that within the 3.5-hour rainfall event, the water table at 1RCH-C rose and fell sharply twice in response to two 15-min periods of high intensity rainfall and an intervening period of less intense rainfall (Plate 1c). Recharge mounds from other rainfall events during March and April dissipated equally quickly.

Seepage faces were rarely observed during the 3-month period of continuous water-level measurements. The water table approached land surface at 1RCH-B only during the March 18 storm, when the lake rose to the elevation of the land surface at this well. Water-level fluctuations due to evapotranspiration were not evident in 15-min data at either the inflow or outflow sites during the data collection period.

Following the largest rainfall events, the water table mound on the inflow side appeared to crest farther inland than

1RCH-C, closer to WTB-19. WTB-19 was located about 19 m from the water's edge, where the unsaturated zone was about 1.4 m thick (see location of WTB-19 and 1PNB-20 on Figure 2). Well 1RCH-C was about 7 m onshore of the water's edge, and the unsaturated zone was about 0.3–0.4 m thick. Weekly and biweekly water-level measurements twice documented a water level at WTB-19 that was higher than the nearshore well 1RCH-C and higher than the basin well located farther onshore (1PNB-20). Measurements were made the day after large rainfall events occurring on March 18, 1996 (6.89 cm), and October 7, 1996 (10.63 cm).

On the outflow side of the lake, water table mounding regularly reversed the outflow head gradient between the lake and 2RCH wells and imposed a steep inflow head gradient (Plate 1b). For the rainfall event on March 18 the water table at 2RCH-C rose 50 cm, peaking about 40 cm above lake stage (Plate 1d). Closer to the lake, at 2RCH-B, the water table rose 15 cm, where it approached land surface and peaked about 8 cm above lake stage. The head in the offshore well 2RCH-A also rose above lake stage, indicating upward flow into the lake in this area. After the storm the water table subsided more slowly than at the inflow side, sustaining the flow reversal for several days.

The five flow reversals that formed on the outflow side of the lake during March 1996 lasted from 1 day to 8 days, depending on the magnitude of the daily rainfall and antecedent water-level conditions (Plate 1b). During March, a month with above average rainfall and a rising water table, all days with rainfall of 0.83 cm or greater caused a flow reversal. In April, which was considerably drier, two larger rainfall events (1.99 cm on April 15 and 3.87 cm rainfall between April 29 and 30) each caused a brief flow reversal in the water table at 2RCH-C that lasted about 12 hours. The latter of the two reversals was evident only in the 15-min data. For the largest rainfall events, water table mounds may have crested inland from 2RCH-C. However, mounding effects were never observed in the closest basin well on the outflow side (2PNB-18, located 34 m onshore from 2RCH-C) (Figure 3). At 2PNB-18 the water table was always 0.4–0.7 m below the level of the lake and the 2RCH wells.

Weekly water-level measurements made over the 15 months from September 1995 to December 1996 periodically documented transient mounding and flow reversals at 2RCH. For example, weekly measurements documented two of the five reversals that were recorded in March by continuous measurements, namely, the two that lasted longest. Flow reversals also were documented in October 1995 and in January, June, and October of 1996. Additional flow reversals undoubtedly occurred during the year but were missed in weekly measurements.

Following the large rainfall events in late March and early October, water table mounding and flow reversals were evident in the basin wells at higher elevations than the RCH wells. Thus, for these events, the ostensible nearshore area to Lake Barco extended farther onshore. Weekly and biweekly water table mapping indicated that these reversals caused inflow head gradients to encircle most of the lake (Figure 5a). In the southern half of the basin, in addition to the 2RCH wells, inflow head gradients also occurred at WTB-13, WTB-6B, and WTB-21 (see well locations on Figure 1a). In these wells the water table depths ranged from 1.5 to 2.5 m. Outflow head gradients also were reversed along the western lake margin at WTB-17, WTB-18, and WTB-22 (water table depths from 2 to 3.2 m).

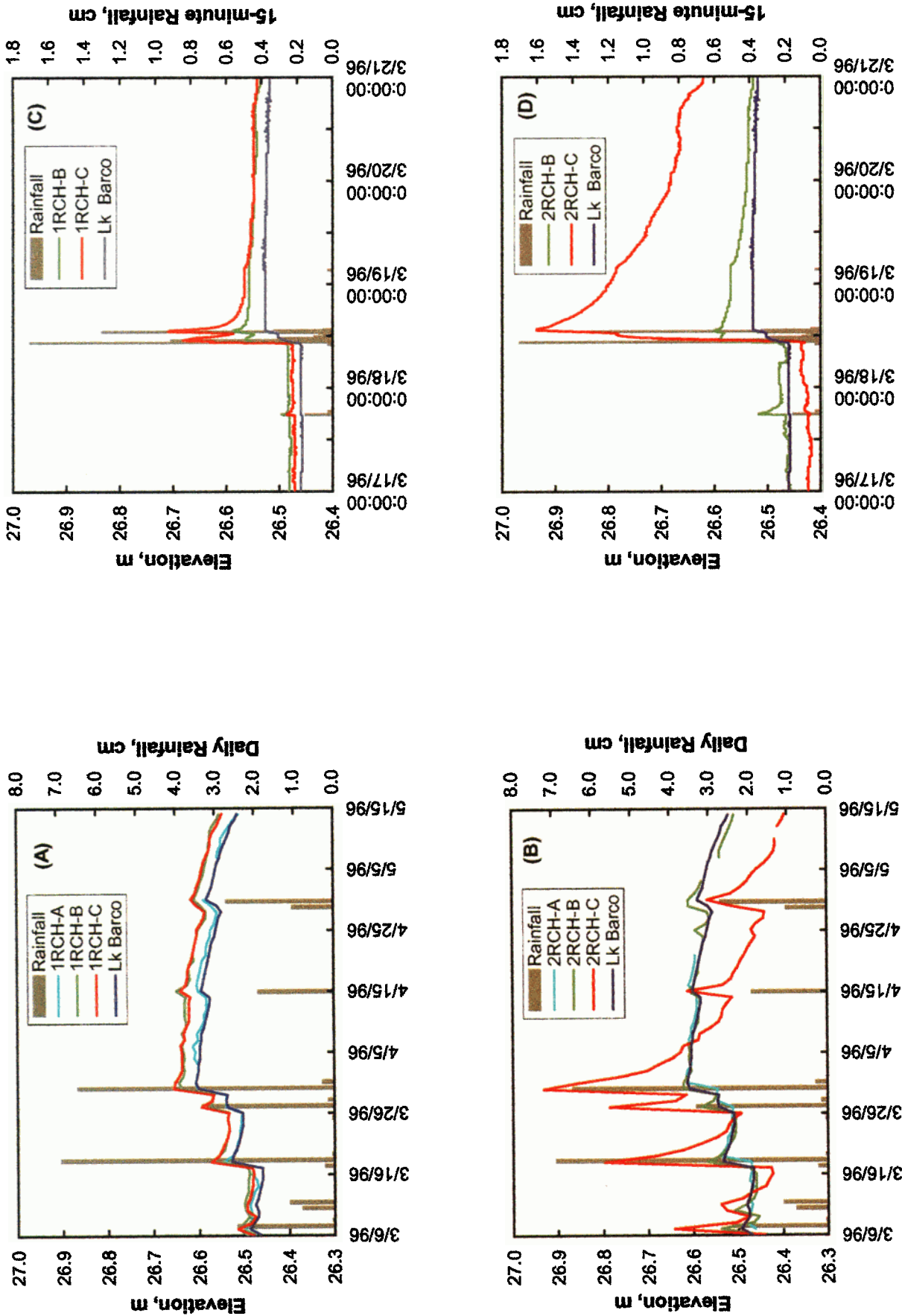


Plate 1. Daily rainfall, daily lake stage in Lake Barco and daily groundwater levels in wells at (a) 1RCH and (b) 2RCH between March 6 and May 15, 1996. The 15-min water levels and rainfall totals at sites (c) 1RCH and (d) 2RCH for a 6.89-cm rainfall event on March 18, 1996.

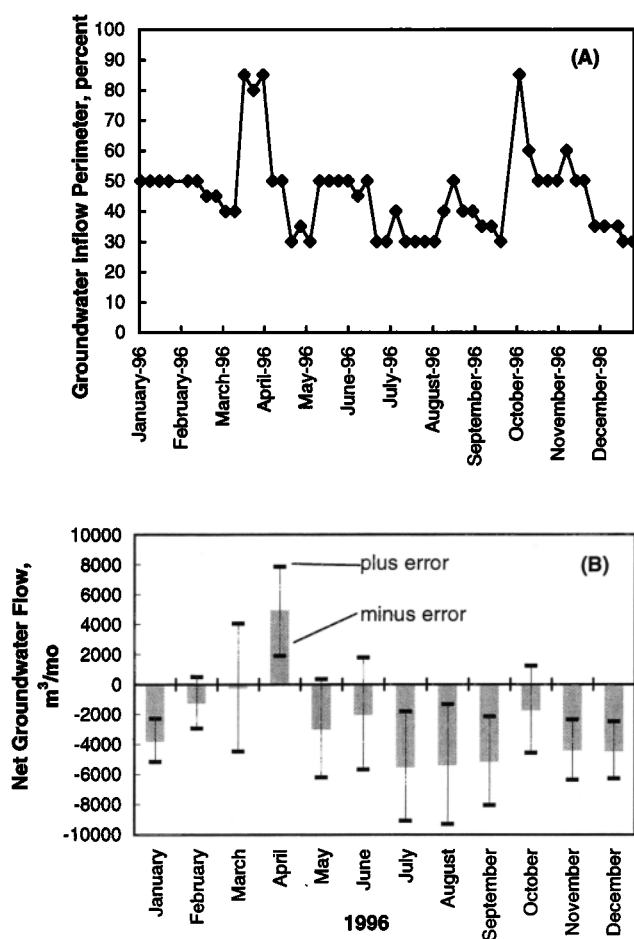


Figure 5. Monthly (a) perimeter of groundwater inflow at Lake Barco for 1996 and (b) net groundwater flow calculated from the lake water budget.

Water table responses in the basin wells farthest from the lake were delayed and moderated by the greater thickness of the unsaturated zone. As a result, the large daily rainfall events in March 1996 generated a single water-level peak apparent in the weekly water-level measurements for wells along the upper inflow hillside. At WTB-1 the peak occurred 3 to 5 weeks after rainfall ended. Near the crest of the ridge at WTB-2 it occurred 6 to 8 weeks later. Because of the lower relief of the outflow hillside, the timing of water-level peaks in WTB-14 and WTB-5 was comparable and occurred about 3 weeks after March rainfall ended.

3.2. Net Groundwater Flow

Net groundwater flow to the lake was computed as the residual term to the monthly water budget equation for Lake Barco. During 1996, net groundwater flow was negative (indicating lake leakage exceeded groundwater inflow or net groundwater outflow) in every month but one (Figure 5b). Groundwater inflow generated during March caused the net groundwater exchange in this month to approach zero. However, a large net groundwater inflow occurred in April, probably in response to the high rainfall at the end of March, including 6.48 cm on March 30. In May, net groundwater exchange was again negative and comparatively large, indicating that the recharge effect from March rainfall was largely completed during April. Most of the groundwater inflow in

April likely occurred in the first part of the month, but this timing cannot be resolved with a monthly water budget.

Net groundwater outflow was greatest between July and September, but it decreased sharply during October because of the groundwater inflow generated by a large recharge event. This groundwater inflow followed a 2-day rainfall event on October 6 and 7 that delivered 13.08 cm of rainfall and caused inflow head gradients around most of the lake margin (Figure 5a). No rain fell during the rest of October, and net lake leakage increased sharply again in November. An apparent decrease in net groundwater outflow in February 1996 was not due to increased inflow but was likely an artifact of overpredicting evaporation in this month. The monthly pan coefficients determined for Lake Barco for 1990 had their largest change of the year between January (0.61) and February (0.78) [Sacks *et al.*, 1994]. However, the timing of spring warming in north Florida can be variable year to year, and using a coefficient between these two values eliminates the appearance of a large decrease in February.

Net groundwater flow was correlated with the percentage of the lake's perimeter having inflow head gradients. During most of 1996, biweekly water table maps plus daily and weekly water-level observations near the lake indicated that between one third and one half of the lake perimeter had inflow head gradients in the adjacent water table. Outflow head gradients existed around the remaining shoreline. During these periods the monthly net groundwater flow was negative (Figure 5b). In March, early April, and early October 1996 the inflow perimeter increased to roughly 90% of the total lake perimeter because of transient flow reversals in the water table adjacent to the lake. Greater groundwater inflow and less lake leakage accompanied the increased inflow perimeter. In April this increase created net groundwater inflow, and in March and October it greatly reduced the net groundwater flow out of the lake.

3.3. Numerical Simulation of Variably Saturated Flow

3.3.1. Steady state flow patterns. The variably saturated flow model simulated the steady state water table position below the inflow and outflow hillsides (Table 1). However, the hydraulic conductivity values in the intermediate confining unit had to be consistently lowered by a factor of about 2 compared to the values used in the saturated groundwater flow model of Lee [1996] (Table 2). The spatial variability of confinement in the basin remained the same, as did the surficial aquifer char-

Table 1. Simulated Steady State Water Table Elevation for Inflow and Outflow Hillside Models

Inflow	1RCH-C	WTB-19	1PNB-20	WTB-1	WTB-2
Steady state ^a	ND	26.90	26.96	31.97	33.71
Simulated	26.86	26.89	27.04	31.93	33.74
Outflow	2RCH-C	2PNB-18	WTB-14	WTB-5	
Steady state ^a	ND	26.15	26.13	26.0	
Simulated ^b	26.58	26.14	26.08	26.02	
Simulated ^c	26.68	26.18	26.11	26.04	

^aSteady state water levels are taken from Lee [1996].

^bValues are simulated with lower conductivity sands near shoreline.

^cValues are simulated with higher conductivity sands near shoreline.

All elevations are in meters above sea level. Lake stage for all cases was 26.83 m above sea level. ND indicates no data.

Table 2. Hydraulic Conductivity Values for Variably Saturated Flow Models

Soil ^a	Hydrogeologic Unit	K_s , m/d
1	SA, upper	0.91
2	SA, lower	0.91
3	lake sediment	0.0182
4	UFA	254
5	SA, inflow nearshore	6.1
6	ICU	0.1
7	ICU	0.4
8	ICU	0.017
9	ICU	0.011
10	SA, outflow nearshore	0.09
11	ICU, outflow hillside	0.37

^aSoil numbers are shown on Figures 2 and 3.

Abbreviations are as follows: SA, surficial aquifer; ICU, intermediate confining unit; UFA, Upper Floridan aquifer; and K_s , saturated hydraulic conductivity.

acteristics. The resulting values were still consistent with the hydrogeologic description of the site [Sacks *et al.*, 1992]. Overall, the intermediate confining unit below the inflow hillside becomes leakier as it gets closer to the karst subsidence feature below the lake. Below the outflow model the intermediate confining unit was uniformly leaky, causing the water table to slope away from this side of the lake (Figures 2 and 3).

On the outflow side of the lake the slope in the water table was steepest between the lake and site 2PNB-18, suggesting a zone of lower horizontal hydraulic conductivity somewhere in this region of the surficial aquifer [Lee, 1996]. The exact loca-

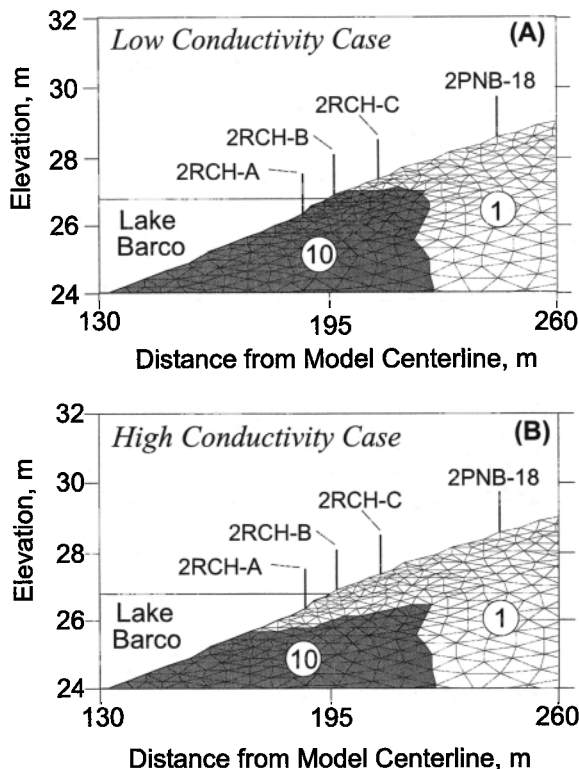


Figure 6. Alternative soil positions near the lake margin of the outflow model: (a) lower-conductivity sand along shallow lake bed and (b) higher-conductivity sand along shallow lake bed.

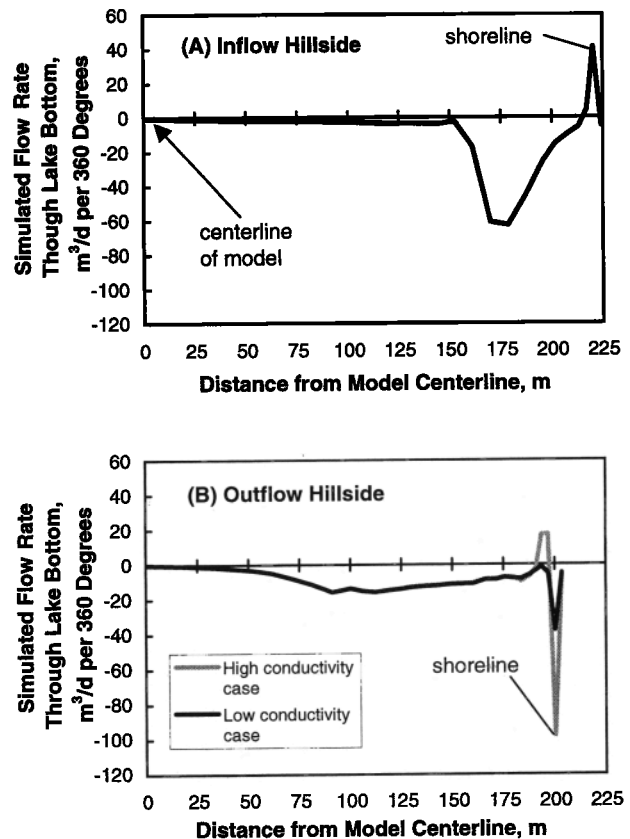


Figure 7. Simulated distribution of inflow and leakage along the lake bottom of (a) the inflow hillside and (b) the outflow hillside for the hypothetical steady state condition.

tion of this zone was not known, so two plausible alternatives were considered to explore their effects on the simulated flows. In the first case a lens of lower-conductivity sand was assumed to exist along the shallow lake bed and extend onshore about 20 m. A cover of more conductive sand overlies the tighter sand (Figure 6a). In the second case the low-conductivity sand lens occurs deeper on the lake bed, about 2 m below the average lake stage, leaving the conductive sand to compose the shallow lake bed (Figure 6b). Both sets of conditions simulated the total head decline between the lake and 2PNB-18. However, the second case provided a better simulation of the small head decline (about 0.1 m) observed between the lake and 2RCH-C (Table 1).

Unlike the staircase geometry of a finite difference grid, the finite element mesh conformed to the gently sloping lake bottom, allowing a detailed simulation of the magnitude and direction of groundwater flow across the lake bed. For the inflow model, for the hypothetical steady state condition, all of the predicted groundwater inflow to the lake occurred within 5 m offshore and at water depths less than 0.4 m (Figure 7a). However, the majority of inflow occurred within 3 m of the shoreline at water depths less than 0.3 m. Leakage occurred through the remainder of the lake bottom. The leakage rate increased with distance offshore and reached a maximum at the deepest part of the lake bottom that was not underlain by organic sediment. Thereafter the leakage rate decreased steeply in response to increasing sediment thickness. Minimal leakage rates occurred across nearly two thirds of the lake

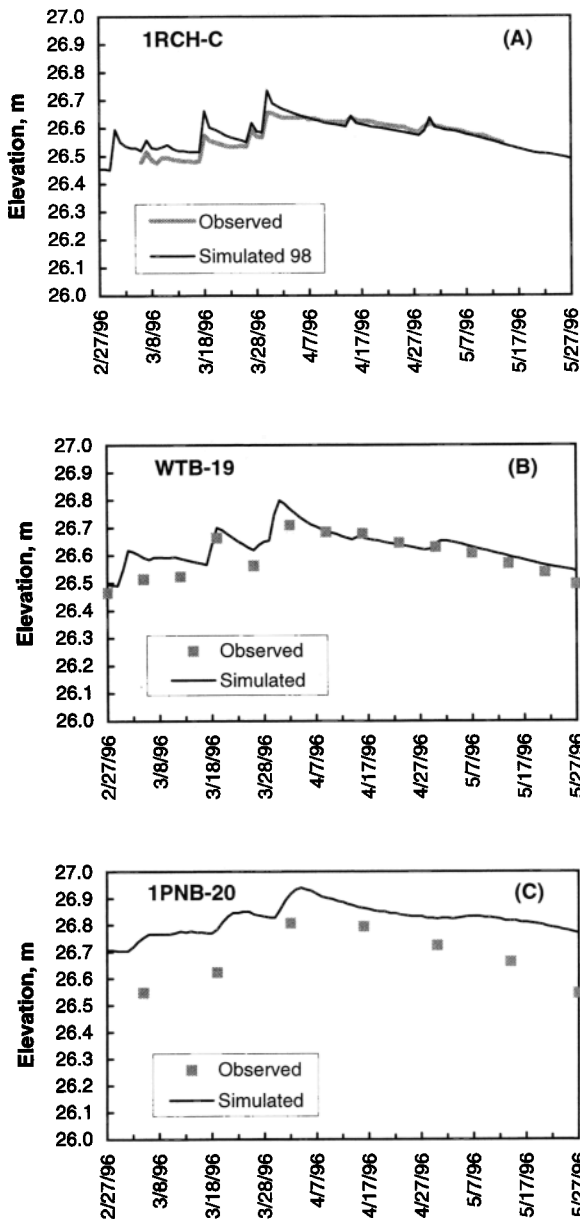


Figure 8. Simulated and observed water levels in wells along the inflow hillside for February 27 through May 27, 1996: (a) 1RCH-C, (b) WTB-19, (c) 1PNB-20, (d) WTB-1, and (e) WTB-2.

bottom where the lake sediment was about 1 m or thicker (Figure 7a).

For the outflow hillside the greatest lake leakage rate occurred at the shallowest lake bed node, regardless of the soil properties assumed for the shallow lake bed. After this shallow peak, leakage decreased sharply with distance offshore. Then it began to increase with depth along the lake bottom, reaching a second peak at the deepest lake bed node that was not underlain by organic sediment (Figure 7b).

For both hillside models the nearshore peak in flow rate into or out of the lake was controlled by the lateral head gradient in the adjacent water table ($\Delta h/\Delta r$) and the horizontal K_s . The deeper peak in leakage rate was controlled by the vertical hydraulic conductivity of the sublake region and the vertical head gradient between the lake and Upper Floridan aquifer

($\Delta h/\Delta z$). Thus leakage increased offshore as the distance (Δz) between the lake and the Upper Floridan aquifer decreased and until the low-permeability sediment was encountered.

This same pattern of fluxes along the lake bed was apparent whether a seepage node was simulated near the shoreline or not. However, the peak flow rate through the shallow lake bed was affected, probably because no recharge can occur through the seepage face. A single seepage node next to the lake on the inflow side decreased the peak groundwater inflow rate through the shallowest lake bed node by about 9%. On the outflow side a seepage node next to the lake increased the peak leakage rate in the shallowest node by about 11 and 6% for the soil arrangements shown in Figures 6a and 6b, respectively.

The geometry of soil properties next to the lake affected the shallow lake leakage through the outflow model. The presence of conductive sands along the shallow lake bed more than doubled the leakage rate compared to the case with low-conductivity sand present (Figure 7b). Further, the presence of higher-conductivity sands in the nearshore region, together with a break in slope along the lake bed, allowed a small amount of the lake leakage to flow back into the lake in the underlying node. The conductive lake bed shown in Figure 6b was used in subsequent simulations because it more accurately simulated the water table between the lake and 2RCH-C.

3.3.2. Transient recharge responses. Transient simulations with the inflow and outflow hillside models were used to explore short-term water table fluctuations near the edge of Lake Barco.

3.3.2.1. Inflow hillside model: The water table profile below the inflow hillside was simulated on a daily basis between

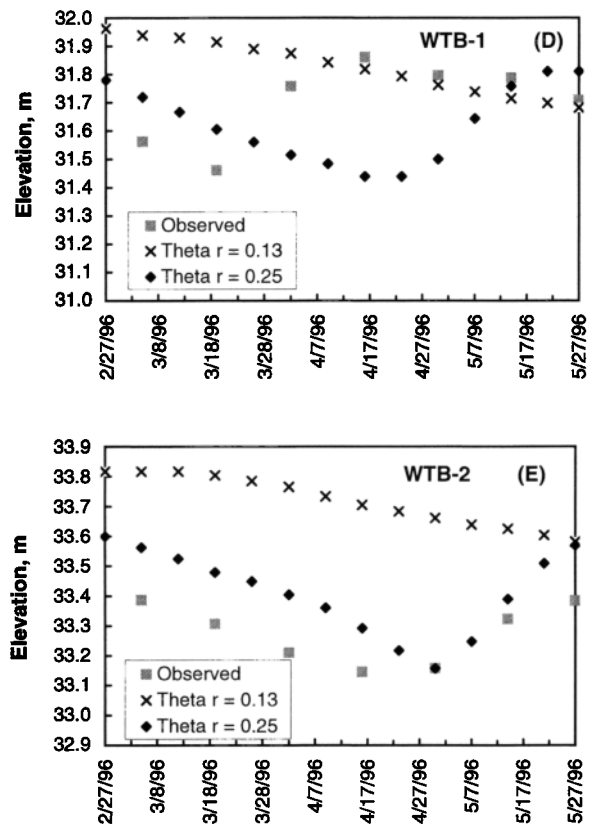


Figure 8. (continued)

February 27 and May 27, 1996. The recharge in the nearshore region was based on simulations from the outflow model (discussed in section 3.3.2.2) and was estimated to be 98% of the daily rainfall, minus daily soil evaporation losses. The simulated water levels showed general agreement with observed water levels along the inflow hillside. However, the agreement was best at 1RCH-C and WTB-19 in the nearshore region. For these sites the model approximated the number of rises in the water table, their timing, and the small changes in the daily water levels. The simulated water levels generally compared within 0.05 m of the observed level (Figures 8a and 8b). Farther from the lake at 1PNB-20, the simulated water level was typically from 0.1 to 0.15 m higher than observed (Figure 8c). However, the model matched the timing and relative magnitude of the principal water-level peak that occurred there in early April.

As anticipated, the short-term water level responses simulated in the upper basin, at wells WTB-1 and WTB-2, showed the poorest agreement with observed levels (Figures 8d and 8e). Differences between simulated and observed water levels in the upper basin at any given time were typically within 0.5 m. The simulated water-level responses in WTB-1 and WTB-2 were sensitive to the hydraulic properties of the unsaturated soil and soil geometry. For example, increasing the thickness of the clayey sands in the lower surficial deposits and raising their residual soil moisture (from 13 to 25%) improved the agreement between the predicted and observed water levels, especially at WTB-2 (Figure 8e). The response also improved at WTB-1; however, the timing of the water table peak still lagged 5 weeks behind the observed peak (Figures 8d). Better information is needed on soil and aquifer hydraulic characteristics and recharge in the upper basin before water levels can be correctly simulated. In these simulations, however, a ± 0.5 -m difference between simulated and observed water levels in the upper basin had negligible effect on heads simulated in the nearshore region.

The simulated groundwater inflow to the lake on the inflow hillside increased immediately in response to daily recharge (Figure 9a). The groundwater inflow rate peaked on the day of rainfall and dropped rapidly afterward. Peak rates were 2 to 4 times higher than the groundwater inflow rates that occurred between rainfall events. The most sustained increase in inflow rate occurred after recharge events on March 18 and 30. The increased inflow due to smaller rain events was limited to one or a few days. Recharge affected the direction and magnitude of flow 10 to 15 m offshore of the lake margin but did not change the leakage rate occurring in deeper nodes along the lake bottom.

Net groundwater exchange with the lake was estimated by summing the positive and negative fluxes along the lake bottom of the inflow hillside (Figure 9b). Net groundwater flow was positive, indicating net inflow, on March 7 and for most of the period from March 18 through April 4. Net leakage was predicted on all but one of the remaining days. Inflow from a rainfall event on April 30 generated a small amount of net groundwater inflow, while inflow on April 15 and 29 reduced the net groundwater outflow.

3.3.2.2. Outflow hillside model: Model results for the outflow hillside were used to provide evidence for the amount of recharge in the nearshore region of both models. Water table mounds dissipated slowly on the outflow side, allowing the outflow hillside model to simulate most of the observed response to recharge at 2RCH-C using daily time periods.

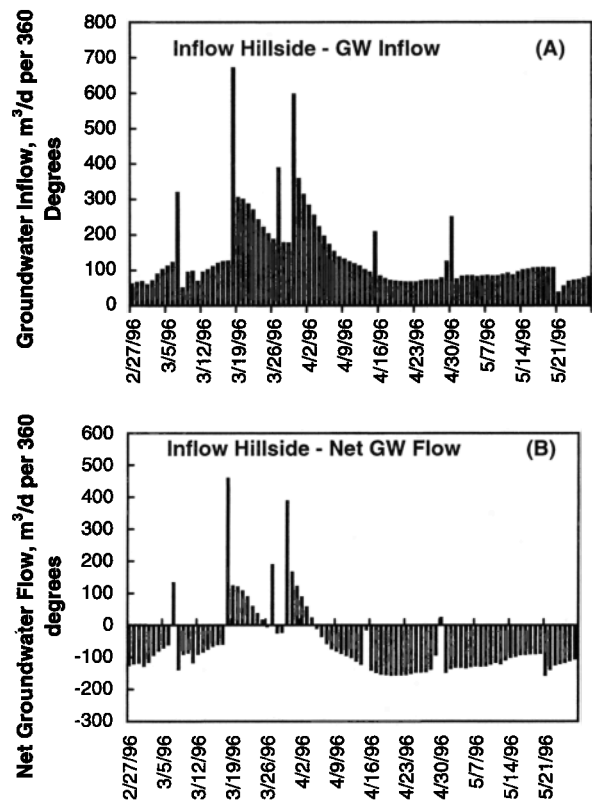


Figure 9. Simulated daily (a) groundwater inflow to Lake Barco and (b) net groundwater exchange with Lake Barco along the inflow hillside for the period February 27 to May 27, 1996.

Thus the simulated water table rise at 2RCH-C was responsive to the rate of recharge applied in the nearshore region and to the soil moisture characteristics in the unsaturated zone in addition to K_s . In contrast, on the inflow side, transient mounds dissipated extremely rapidly, and the simulated daily water levels on the inflow side at 1RCH-C were relatively unresponsive to the recharge or specific yield assumed. Instead, the model simulated the recovered water table position after storms and was more responsive to lake stage and K_s .

Water levels beneath the outflow hillside were simulated on a daily basis between February 27 and May 27, 1996. Reproducing the transient water table mounds and flow reversals observed on the outflow side of Lake Barco required that the majority of the daily rainfall be used to recharge the water table in the nearshore region. Approximating daily recharge as 87% of daily rainfall minus the daily evaporation loss simulated only the groundwater flow reversal on March 30 (Figure 10a). The simulation improved if the specific yield of soils in the nearshore region were reduced by raising the residual soil moisture content (θ_r) from 3 to 17% (Figure 10b). However, the simulated flow reversals at 2RCH-C were shorter-lived than the observed reversals, and the water levels following recharge fell below the observed levels. Decreasing daily recharge to 65% of the daily rainfall was inadequate for simulating flow reversals even when θ_r was raised to 17% (Figure 10b).

The transient water level responses at 2RCH-C were more closely simulated when the nearshore recharge was increased to 98% of the daily rainfall minus the daily evaporation loss,

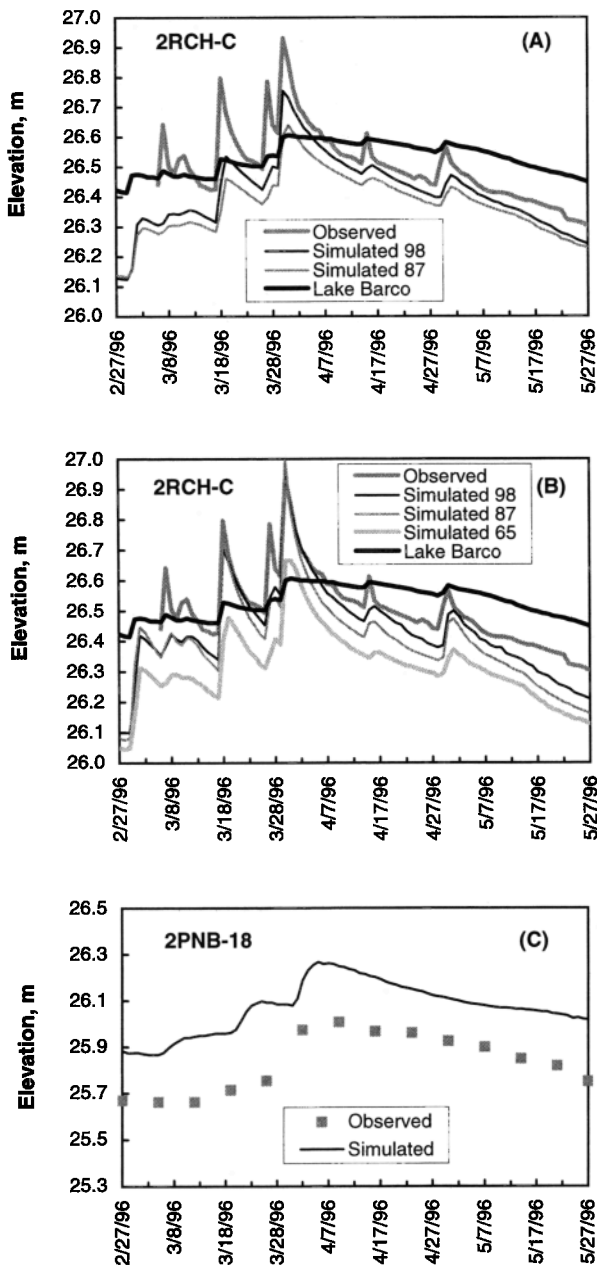


Figure 10. Simulated and observed water levels in wells along the outflow hillside for February 27 through May 27, 1996: (a) 2RCH-C with recharge based on 98 and 87% of the daily rainfall and θ_r equal to 3%, (b) 2RCH-C with recharge based on 98% of the daily rainfall and θ_r equal to 12% and with recharge based on 87 and 65% of the daily rainfall with θ_r increased to 17%, (c) 2PNB-18, (d) WTB-14, and (e) WTB-5.

and θ_r was increased to 12% (compare Figures 10a and 10b). The recession rate of the water level following the peak was reasonably well matched suggesting that the dissipation rate of the mound by saturated flow was appropriate. Further, the position of the water table between recharge events was closer to the observed levels at 2RCH-C, also suggesting the amount of recharge was appropriate. The majority of the daily rainfall from the large storms appears to be involved in the daily recharge; however, determining the exact rate of nearshore recharge would require more detailed analysis and data collection. For the modeling analysis in this study, daily recharge

was based upon 98% of the daily rainfall applied in the nearshore region. The residual moisture content in the nearshore region of the outflow hillside was increased to 12%.

The outflow hillside model simulated the steeper and more persistent water table mounding near the edge of the lake in contrast to the inflow side (Figure 10b). It also simulated the lagged response of the upper basin wells (Figures 10c, 10d, and 10e). Yet on several occasions mounding that was observed at 2RCH-C was not simulated by the model, and simulated mounds were often closer to the lake than observed. For example, on March 27 the apex of the simulated mound was closer to 2RCH-B than to 2RCH-C. The model did not simulate the water table mounding and flow reversals observed at 2RCH-C for the two earliest storms in March, although flow reversals were simulated at 2RCH-B. This may have been attributable to the fact that the initial simulated water table at 2RCH-C was about 0.1 m lower than the observed level. By increasing the depth of the capillary fringe below land surface, the lower water table at 2RCH-C may have contributed to the lower simulated response [e.g., *Novakowski and Gillham, 1988*]. On March 30, when the simulated water table was near the observed level, the predicted response at 2RCH-C agreed more closely with the observed water level peak.

A representative flow reversal simulated near the outflow side of the lake for March 30, 1996, is shown in Figure 11. On the previous day (March 29) the water table sloped away from the lake, although less steeply than usual because of a storm 2 days earlier. Recharge on March 30 created a mound in the water table between the lake and 2RCH-C that reversed the head gradient and generated groundwater inflow through the shallow lake bottom. Most of the simulated inflow occurred

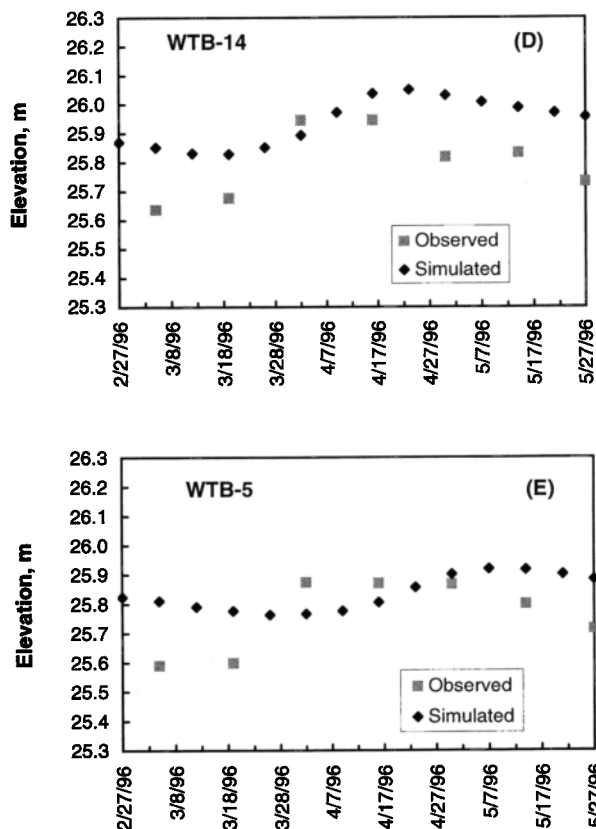


Figure 10. (continued)

within 3 m offshore in water less than 0.2 m deep. Two days later on April 1, the mound had flattened out and moved onshore as the permeating wetting front intercepted the water table farther from the lake. Mounding below the hillside ceased at the point where the thickness of the unsaturated zone slowed the rate of recharge below the rate of redistribution. The simulated mound and flow reversal from the March 30 rainfall lasted for 5 days (Figure 11).

The simulated flow reversals on the outflow hillside generated groundwater inflow to the lake (Figure 12a). Inflow was always shallow, and flow rate and direction were affected only in the shallowest nodes in the lake bed. The largest inflow rate occurred on the day of rainfall, and inflow decreased exponentially on subsequent days. The longest simulated period of groundwater inflow to the lake lasted 4 days and followed the storm on March 30 (Figure 12a). Mounding also increased the groundwater lost to evaporation along the land surface near the lake. Flow reversals (at 2RCH-B) on April 15 and 30 also generated inflow. The small inflow amounts predicted on other days in April and May resulted from lake leakage that circulated back into the lake. Increasing θ_r in the nearshore region from 3 to 12% increased the groundwater inflow associated with flow reversals and increased inflow over the 3-month simulation period by about 20%. However, outflow between storms increased slightly causing a similar net flow rate for the two values of θ_r .

Between rainstorms the net groundwater flow was uniformly large and negative indicating net leakage along the lake bottom of the outflow section, regardless of the soil properties assumed near the lake margin (Figure 12b). Net groundwater outflow through the outflow side of the lake occurred at about twice the rate as that on the inflow side of the lake. Inflow generated by nearshore recharge briefly but significantly reduced the net leakage along the lake bottom. With low-conductivity soil adjacent to the shallow lake bed, the groundwater inflow generated by flow reversals was small and served only to decrease the net leakage, typically by 30% or less. With higher conductivity sand along the shallow lake bed the groundwater inflow occasionally approached the sum of the

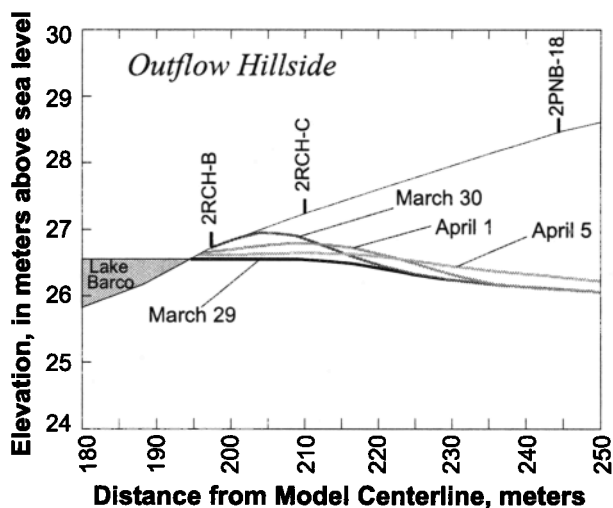


Figure 11. Outflow hillside showing a transient water table mound simulated for a 6.48-cm rainfall event on March 30, 1996 (assumes θ_r equals 3% in nearshore region as in Figure 10a).

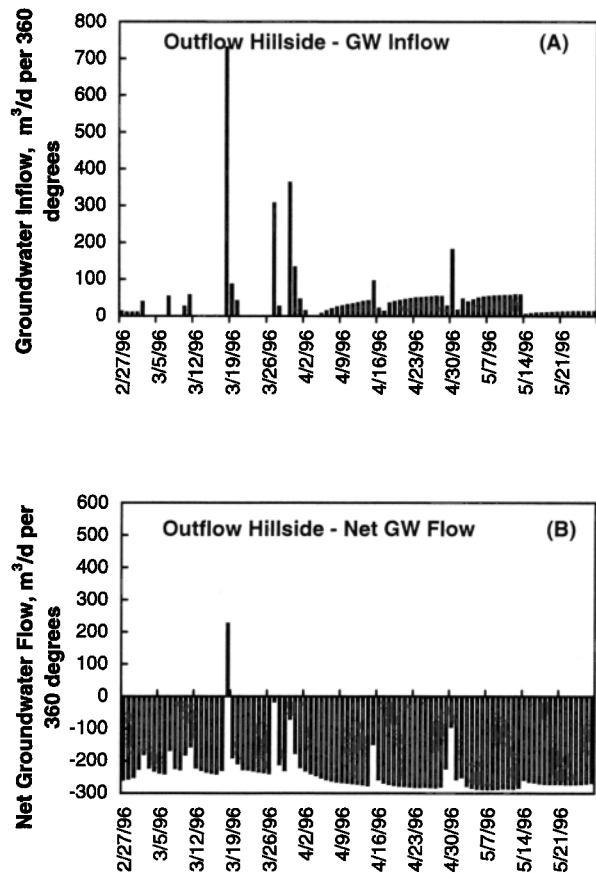


Figure 12. Simulated daily (a) groundwater inflow to Lake Barco and (b) net groundwater exchange with Lake Barco along the outflow section for the period February 27 to May 27, 1996.

leakage through the remaining lake bottom, causing the net flow to approach zero (Figures 12a and 12b). The largest daily groundwater inflow occurred on March 18, following a storm comparable to the one on March 30. It generated a large net groundwater inflow from the outflow hillside.

3.3.3. Comparison of simulated and budget-derived net groundwater flow. Although both approaches contain large levels of uncertainty, a rudimentary comparison of the model-derived and water budget-derived estimates of net groundwater flow was made to complete the approach. The greatest amount of simulated groundwater inflow occurred between March 15 and April 15, 1996. For this same time period, net groundwater flow derived from the lake water budget was $6170 \pm 3500 \text{ m}^3$ (which exceeds the net inflow attributable solely to the month of April in Figure 5b). During this period, about 90% of the perimeter of the lake was experiencing groundwater inflow (Figure 5a). If we assume the inflow hillside gives an apt description of the entire circumference of the lake, the simulated net groundwater flow to the lake for this 1-month period would be 1040 m^3 .

During May 1996, the driest part of the 3-month simulation period, inflow occurred at about 40% of the lake perimeter, and outflow occurred from the remaining 60% (Figure 5a). If we prorate the modeled fluxes from the inflow hillside and the outflow hillside to the entire lake using these percentages, the model-simulated net groundwater flow (net lake leakage) for

May would be -5620 m^3 . The net groundwater flow derived from the lake water budget for May was $-2930 \pm -3270 \text{ m}^3$.

4. Discussion

Simulating variably saturated groundwater flow processes in the basin expands our understanding of groundwater interactions with Lake Barco well beyond the previous saturated flow modeling results of Lee [1996]. Although the results in the study are preliminary in nature, the variably saturated groundwater flow model simulated the transient water table mounding and groundwater flow reversals observed near the edge of Lake Barco, together with the slower recharge occurring in the upper basin. Model results indicated that transient water table mounding in the nearshore region was the process generating net groundwater inflow to Lake Barco during March and April 1996. The lake water budget confirmed the occurrence of net groundwater inflow to the lake within March and April.

The generation of net groundwater inflow to Lake Barco by transient mounds was mainly the result of large daily rainfall events, not a succession of smaller events. Antecedent rainfall appeared to be less important to the generation of inflow than antecedent water table elevation in the nearshore region and the magnitude of daily rainfall. Most of the simulated groundwater inflow was from the inflow hillside. However, depending upon the soil geometry near the lake, flow reversals on the outflow hillside had the potential to generate a substantial amount of groundwater inflow. Simulated groundwater inflow from both hillsides was always greatest on the day of the rainfall event and declined exponentially thereafter.

Modeling results indicate that on rainy days, recharge for the sandy nearshore region was a majority of the daily rainfall and could be upward of 87% of the daily rainfall minus the evaporation from the land surface. Realistic transient flow reversals on the outflow side of the lake were not simulated at lesser recharge rates even under a range of plausible soil characteristics that would promote mound formation. In the upper basin, defined to be where the water table depth was greater than 2.5 m below land surface, the recharge rate to the surficial aquifer was much lower than in the nearshore region. Ideally, recharge rates should differ along the hillside as a function of unsaturated zone thickness. However, the model allowed one time-varying specified flux boundary and one atmospheric boundary to be applied along the emergent hillside; therefore a single higher recharge rate was used for the nearshore region. Using the higher "nearshore" recharge where the water table depth was between about 1.5 m and 2.5 m probably explains why water levels simulated for 1PNB-20 and 2PNB-18 were consistently higher than observed.

Variably saturated flow modeling and the lake water-budget analysis yielded similar results on the timing of net groundwater inflow to the lake, but the model-simulated net groundwater inflow was perhaps 5 times lower than the water-budget-derived estimate for the period March 15 to April 15. This occurs despite the high recharge rate simulated for the nearshore region. Some difference between the two results is expected considering the numerous simplifications inherent in the comparison. For one, the conditions simulated along the two hillsides cannot accurately represent the entire lake perimeter. However, other limitations of the modeling may contribute to the smaller simulated inflow.

The smaller quantity of modeled inflow likely reflects the tendency of the model to simulate a nearshore region that was

smaller than observed on the outflow hillside and also possibly on the inflow hillside. In general, on the day of the rainfall event the observed water table mounds on the outflow hillside were larger in breadth and centered farther from the lake than mounds simulated by the hillside model. In model simulations the water table mound crested at 2RCH-C a day after the observed water table peak. The model may simulate a slower water table response because of the moisture characteristics assumed for the soil or the time discretization of the recharge or because it does not account for some preferential vertical flow. On the inflow hillside the mound center was typically simulated between 1RCH-C and WTB-19, but its exact location could not be determined because the rapid saturated flow greatly flattened out the peak. For the largest rainfall events, water levels measured in basin wells indicated that transient groundwater mounding and flow reversals could occur farther from the lake than the 1RCH and 2RCH wells in areas where the unsaturated zone is between 1 and 3 m.

Flow reversals occurring on the outflow hillside probably lasted longer, and generated more groundwater inflow to the lake, than the simulated counterpart. The longest simulated period of groundwater inflow from the outflow hillside lasted 4 days and followed a daily rainfall event of 6.48 cm on March 30. Seepage meter measurements made later in the study indicated that the period of groundwater inflow could last much longer than 4 days. For example, 14 days after a 10-cm rainfall event on October 7, 1996, groundwater inflow was measured in replicate seepage meters placed next to 2RCH-A (S. Sigler, Department of Oceanography, Florida State University, written communication, November 1996). Longer-lasting flow reversals would increase net groundwater inflow to the lake both by generating greater groundwater inflow and by inhibiting lake leakage near the shoreline. On the inflow hillside the predicted groundwater inflow to the lake would increase if recharge was simulated over shorter time periods and the steep, short-term water table mounding was reproduced. However, simulating the short-lived and steep inflow head gradients associated with the intensive rainfall would require the use of short boundary periods (e.g., 15 min) that would likely complicate numerical convergence in the model.

In model simulations using daily boundary periods, differences in K_s alone were sufficient to explain much of the observed differences in daily water levels on the two sides of the lake. The rapid dissipation of the mound on the inflow side was consistent with the greater hydraulic conductivity in the surficial aquifer at 1PNB-20. At the outflow side the higher daily water level and slower decline was evidence of significantly lower K_s in the surficial aquifer near the lake. Simulating the instantaneous water table peaks (observed in continuous water level data) was not possible using daily boundary periods. However, simulating instantaneous peaks would improve the capacity of the model to test hypotheses about soil moisture characteristics.

Ignoring transpiration in the nearshore region contributes an additional source of error to the analysis but should not greatly effect the groundwater fluxes predicted on the day of rainfall or for a day or two thereafter. In the brief time between recharge to the water table and discharge to the lake, transpiration losses should be small compared to the magnitude of recharge. On dry days, transpiration effects should reduce the calculated groundwater inflow on the inflow side and increase the simulated lake leakage rate on the outflow side compared to the present results.

Modeling results were subject to uncertainties in the spatial distribution of recharge rates and soil physical characteristics already mentioned, as well as other simplifying assumptions. In the unsaturated zone the effects of hysteresis, anisotropy, and preferential flow paths were ignored. An additional source of uncertainty stems from the assumption of radial symmetry around the lake for each of the model sections; however, this approach is preferable over a 2-D cross section [Winter, 1978]. Modeling results were not tested for their sensitivity to the dimensions of the grid or to the mesh distortion. Recent results by Paniconi and Wood [1993] suggest that the grid distortion used here should not be problematic. Finally, the head in the Upper Floridan aquifer remained constant in the model. This simplification was suitable for the simulation of Lake Barco. However, it would not suffice farther south in the Central Lake District where the downward head gradient in the surficial aquifer can change over time because of groundwater pumping from the Upper Floridan aquifer.

The mantled karst terrain and humid climate of central Florida could magnify the relative importance of nearshore recharge to the water budget of Lake Barco and similar lakes. Although the surficial deposits are reasonably conductive, the karst hydrogeologic setting limits the size of the groundwater basin contributing inflow to Lake Barco. The role of the nearshore region of the contributing basin may be heightened both because it receives the most efficient short-term recharge and because discharge from this part of the surficial aquifer has the greatest likelihood of entering the lake. Nearshore recharge is also important because it is the only process contributing inflow and inhibiting leakage along the large outflow perimeter of Lake Barco. In general, groundwater inflow generated by nearshore recharge should effect the water budget of small seepage lakes, or lakes with lobate shorelines, more than larger lakes of comparable depth [Millar, 1971]. Similarly, shallow lakes should be relatively more affected than deep lakes [e.g., Winter and Pfannkuch, 1984]. Small, shallow, flow-through lakes are relatively commonplace in Florida [Brenner et al., 1990; Sacks et al., 1998], as well as in glacial terrain [Born et al., 1979]. For lakes in these settings the hydrology of the nearshore region deserves greater attention.

The literature on basin recharge is often fragmented by descriptions that categorize subsurface hydrologic processes spatially (i.e., as being in the nearshore area, in recharge or discharge areas, in areas with a shallow, intermediate, or deep water table, etc.) and temporally (i.e., by the longevity or transience of the water table configuration). Yet such categories can be indefinite because successive rainfall events shift both the timing and spatial distribution of the recharge and water table responses. This fragmentation reflects our current inability to envision and simulate basin recharge processes on the whole. With increased application of variably saturated flow models such descriptions of unsteady water table configurations should gradually give way to a more integrated understanding of the nature of groundwater recharge and discharge throughout lake basins.

5. Conclusions

The following conclusions may be drawn from this study:

1. For Lake Barco and similar lakes in mantled karst terrain, rapid and efficient nearshore recharge, and the transient groundwater flow patterns it generates, may be a significant source of groundwater inflow from both the inflow and outflow

sides of the lake. Further, it may be the process that is most effective at generating net groundwater inflow.

2. Variably saturated groundwater flow modeling can be used to simulate transient water table mounding and flow reversals in permeable aquifers near lakes in humid climates. Variably saturated flow modeling is best used in conjunction with lake water budgets and field data to explore groundwater recharge and discharge for lake basins. Until field studies can fully describe the physical characteristics of the unsaturated zone and independently quantify recharge rates, modeling will remain largely conceptual, and the results will be semiquantitative. However, modeling provides a tool for testing hypotheses about the effects of topography, soils, climate, and hydrogeology on the nature of lake and groundwater interactions.

3. Transient water table mounding probably commonly occurs near lakes located in permeable terrain. However, water table responses to rainfall can be rapid, and documenting them may require frequent water-level measurements close to the lake.

4. To better understand the water budgets of certain lakes in mantled karst terrain, it is necessary to include the distinctive groundwater flow processes of the nearshore region along with the larger-scale groundwater flow.

Acknowledgments. This work was supported by funding from the U.S. Geological Survey, the Southwest Florida Water Management District, and the St. John's River Water Management District. The Katharine C. Ordway Preserve Management Advisory Board granted access to Lake Barco, and the site caretaker, T. Perry, provided much practical guidance for working on the preserve. The author is especially grateful for the assistance of site observer I. Prentice, whose excellent data collection made the study possible, to R. Healy and D. Sumner for helpful early insights on the project, and to J. Šimůnek for assistance with the model.

References

- Anderson, M. P., and J. A. Munter, Seasonal reversal of groundwater flow around lakes and the relevance to stagnation points and lake budgets, *Water Resour. Res.*, 17(4), 1139–1150, 1981.
- Arrington, D. V., and R. C. Lindquist, Thickly mantled karst of the Interlachen area, in *Proceedings of Second Multidisciplinary Conference on Sinkholes and the Environmental Impacts of Karst*, edited by B. F. Beck and W. L. Wilson, pp. 31–39, Fl. Sinkhole Res. Inst., Orlando, Fla., 1987.
- Born, S. M., S. A. Smith, and D. A. Stephenson, Hydrogeology of glacial-terrain lakes, with management and planning applications, *J. Hydrol.*, 43, 7–43, 1979.
- Brenner, M., M. W. Binford, and E. S. Deevey, Jr., Lakes, in *Ecosystems of Florida*, edited by R. L. Myers and J. E. Ewel, pp. 368–391, Univ. of Cent. Fla. Press, Orlando, 1990.
- Brooks, H. K., *Physiographic Divisions of Florida*, Univ. of Fla. Cent. for Environ. and Nat. Resour., Gainesville, 1981.
- Freeze, R. A., Three-dimensional, transient, saturated-unsaturated flow in a groundwater basin, *Water Resour. Res.*, 7(2), 347–366, 1971.
- Griibb, M. M., and G. Sewell, Solution of ground water flow problems with general purpose and special purpose computer codes, *Ground Water*, 36(2), 366–372, 1998.
- Katz, B. G., T. M. Lee, N. L. Plummer, and E. Busenberg, Chemical evolution of groundwater near a sinkhole lake, northern Florida, 1, Flow patterns, age of groundwater, and influence of lake water leakage, *Water Resour. Res.*, 31(6), 1549–1564, 1995.
- Knowles, L., Jr., Estimation of evapotranspiration in the Rainbow Springs and Silver Springs basins in north-central Florida, *U.S. Geol. Surv. Water Resour. Invest. Rep.*, 96–4024, 1996.
- Krabbenhoft, D. P., and K. E. Webster, Transient hydrogeological controls on the chemistry of a seepage lake, *Water Resour. Res.*, 31(9), 2295–2305, 1995.
- Lee, T. M., Hydrogeologic controls on the groundwater interactions

- with an acidic lake in karst terrain, Lake Barco, Florida, *Water Resour. Res.*, 32(4), 831–844, 1996.
- Lee, T. M., and A. Swancar, Influence of evaporation, ground water, and uncertainty in the hydrologic budget of Lake Lucerne, a seepage lake in Polk County, Florida, *U.S. Geol. Surv. Water Supply Pap.*, 2439, 1997.
- Meayboom, P., Unsteady groundwater flow near a willow ring in hummocky moraine, *J. Hydrol.*, 4, 38–62, 1966.
- Millar, J. B., Shoreline-area ratio as a factor in rate of water loss from small sloughs, *J. Hydrol.*, 14, 259–284, 1971.
- Mills, J. G., and M. A. Zwarich, Transient groundwater flow surrounding a recharge slough in a till plain, *Can. J. Soil Sci.*, 66, 121–134, 1986.
- National Oceanic and Atmospheric Administration, Climatological data annual summary, Florida, *Rep. 100*, (13), U.S. Dep. of Commer., Washington, D. C., 1996.
- Novakowski, K. S., and R. W. Gillham, Field investigations of the nature of water-table response to precipitation in shallow water-table environments, *J. Hydrol.*, 97, 23–32, 1988.
- Paniconi, Cl., and E. F. Wood, A detailed model for simulation of catchment scale subsurface hydrologic processes, *Water Resour. Res.*, 29(6), 1601–1620, 1993.
- Pollman, C. D., T. M. Lee, W. J. Andrews, L. A. Sacks, S. A. Gherini, and R. K. Munson, Preliminary analysis of the hydrologic and geochemical controls on acid-neutralizing capacity in two acidic seepage lakes in Florida, *Water Resour. Res.*, 27(9), 2321–2335, 1991.
- Potter, S. T., and W. J. Gburek, Variably-saturated finite-element model for hillside investigations, in *Computational Methods in Water Resources: Proceedings of the VII International Conference* vol. 1, *Modeling Surface and Sub-surface Flows*, pp. 127–132, Elsevier Sci., New York, 1988.
- Readle, E. L., Soil survey of Putnam County area, Florida, report, Univ. of Fla., Gainesville, March 1990.
- Rosenberry, D. O., and T. C. Winter, Dynamics of water-table fluctuations in an upland between two prairie-pothole wetlands in North Dakota, *J. Hydrol.*, 191, 266–289, 1997.
- Sacks, L. A., T. M. Lee, and A. B. Tihansky, Hydrogeologic setting and preliminary data analysis for the hydrologic-budget assessment of Lake Barco, an acidic seepage lake in Putnam County, Florida, *U.S. Geol. Surv. Water Resour. Invest. Rep.*, 91–4180, 1992.
- Sacks, L. A., T. M. Lee, and M. J. Radell, Comparison of energy-budget evaporation losses from two inorphometrically different Florida seepage lakes, *J. Hydrol.*, 156, 311–334, 1994.
- Sacks, L. A., A. Swancar, and T. M. Lee, Estimating ground-water exchange with lakes using water-budget and chemical mass-balance approaches for ten lakes in ridge areas of Polk and Highlands Counties, Florida, *U.S. Geol. Surv. Water Resour. Invest. Rep.*, 98–4133, 1998.
- Salvucci, G. D., and D. Entekhabi, Hillside and climatic controls on hydrologic fluxes, *Water Resour. Res.*, 31(7), 1725–1739, 1995.
- Scott, T. M., The Hawthorn Formation of northeastern Florida, part I, The geology of the Hawthorn Formation of northeastern Florida, *Rep. Invest. Fla. Bur. Geol.*, 93, 1983.
- Šimůnek, J., M. Sejna, and M. T. van Genuchten, The SWMS-2D code for simulating water flow and solute transport in two-dimensional variably-saturated media, version 1.1, *Res. Rep. 126*, 169 pp., U.S. Salinity Lab., Agric. Res. Serv., U.S. Dep. of Agric., Riverside, Calif., 1992.
- Šimůnek, J., T. Vogel, and M. T. van Genuchten, HYDRUS-2D simulating water flow and solute transport in two-dimensional variably-saturated media, *IGWMC-TP 53*, version 1.0, Int. Ground Water Model. Cent., Colo. Sch. of Mines, Golden, January 1996.
- Stolte, W. J., S. L. Barbour, and R. G. Eilers, A simulation of the mechanisms influencing salinity development around prairie sloughs, in *Aquatic Ecosystems in Semi-Arid Regions: Implications for Resource Management*, *NHRI Symp. Ser.*, edited by R. D. Roberts and M. L. Bothwell, pp. 165–177, Environ. Can., Saskatoon, Saskatchewan, 1992.
- Sumner, D. M., Evapotranspiration from an area of successional vegetation in a deforested area of the Lake Wales Ridge, Florida, *U.S. Geol. Surv. Water Resour. Invest. Rep.*, 95–4244, 1996.
- Sumner, D. M., and L. A. Bradner, Hydraulic characteristics and nutrient transport and transformation beneath a rapid infiltration basin, Reedy Creek Improvement District, Orange County, Florida, *U.S. Geol. Surv. Water Resour. Invest. Rep.*, 95–4281, 1996.
- van Genuchten, M. T., F. J. Leij, and S. R. Yates, The RETC code for quantifying the hydraulic functions of unsaturated soils, *Rep. EPA/600/2-91/065*, 85 pp., Environ. Prot. Agency, Washington, D. C., December 1991.
- Winter, T. C., Numerical simulation of steady state three-dimensional ground-water flow near lakes, *Water Resour. Res.*, 14(2), 245–254, 1978.
- Winter, T. C., The interaction of lakes with variably saturated porous media, *Water Resour. Res.*, 19(5), 1203–1218, 1983.
- Winter, T. C., Conceptual framework for assessing cumulative impacts on the hydrology of nontidal wetlands, *Environ. Manage.*, 12(5), 605–620, 1988.
- Winter, T. C., and H. O. Pfannkuch, Effect of anisotropy and ground-water system geometry on seepage through lakebeds, 2, Numerical simulation analysis, *J. Hydrol.*, 75, 239–253, 1984.
- Winter, T. C., and D. O. Rosenberry, The interaction of ground water with prairie pothole wetlands in the Cottonwood Lake area, east-central North Dakota, 1979–1990, *Wetlands*, 15(3), 193–211, 1995.
- Wu, J., R. Zhang, and J. Yang, Analysis of rainfall-recharge relationships, *J. Hydrol.*, 177(1–2), 143–160, 1996.

T. M. Lee, Water Resour. Division, U.S. Geological Survey, 4710 Eisenhower Blvd., Suite B-5, Tampa, FL 33634-6381. (tmlee@usgs.gov)

(Received January 19, 2000; revised April 12, 2000; accepted April 12, 2000.)